# Tuning and Costs Analysis for a Trajectory Planning Algorithm for Autonomous Vehicles

Abdallah Said, Reine Talj, Clovis Francis, Hassan Shraim

# Tuning and Costs Analysis for a Trajectory Planning Algorithm for Autonomous Vehicles

Abdallah Said[1,2], Reine Talj[1], Clovis Francis[2] and Hassan Shraim[2]

[1]*Université de Technologie de Compiègne, CNRS, Heudiasyc (Heuristics and Diagnosis of Complex Systems), CS 60 319, 60 203 Compiègne Cedex, France*

[2]*Université Libanaise, Faculté de Génie, Centre de Recherche Scientifique en Ingénierie (CRSI), Liban*

*(abdallah.said, reine.talj)@hds.utc.fr, (cfrancis, hassan.shraim) @ul.edu.lb*

Keywords: Autonomous vehicle, trajectory planning, cost analysis

Abstract: Trajectory planning is an essential issue for autonomous vehicles navigation. It represents a decision-making level that considers several constraints to be respected to navigate safely and comfortably in a dynamic environment. This paper presents a reactive trajectory planning, which consists to generates several candidate trajectories. Then, selecting the best trajectory among candidates is based on different criteria, each described by a cost function. Indeed, the algorithm aims to minimize a global cost function, a combination of several costs, to determine the best trajectory. The main objective of this work is to study the algorithm's sensitivity against parameter tuning and to find a generic range of weighting coefficients for the cost function of the planning algorithm to make the algorithm as reliable as possible against various driving conditions.

## 1 INTRODUCTION

An autonomous vehicle needs a local trajectory based on real-time vehicle status and dynamic environment perception data (e.g., nearby cars, road conditions) to guarantee safe maneuvers while following the global trajectory. Local trajectory planning is defined as the planning of a vehicle's transition from one possible state to the next one while satisfying the vehicle's kinematic restrictions based on the vehicle dynamics and constrained by the passenger's comfort, lane boundaries, and traffic rules while avoiding static and dynamic obstacles. Different trajectory planning approaches have been developed for the navigation of autonomous vehicles (Dixit et al., 2018), (Katrakazas et al., 2015). They differ in how they deal with the environment and the vehicle dynamics limitations. According to the literature, there are four well-known approaches to trajectory planning methods: grids generalization (Pivtoraiko and Kelly, 2005), sampling-based planning (Karaman and Frazzoli, 2011), numerical optimization methods (Lim et al., 2018) and curve interpolation methods (Alia et al., 2015). The last approach is adopted, and it aims to generate trajectories on a given horizon with a specified geometric shape that responds to one or more constraints such as vehicle dynamics and kinematics, comfort, road shape, and curvature continuity. Each candidate trajectory is assessed using a cost function that takes into account several factors such as traveled distance and execution time costs, acceleration, collision verification, and other performance criteria. Then, the cost function is minimized to find the best trajectory among several candidate trajectories generated by the planning algorithm. Each one of these costs is multiplied by a weighting coefficient to rank its significance. The major weakness of this approach is that, for some trajectory shapes, the result of the planning algorithm is highly dependent on the tuning of the cost weights . Moreover, function of the shape of geometric curves, which represent candidate trajectories, the algorithm is more or less dependent on tuning weights. It is important to evaluate the sensitivity of the planning algorithm to the tuning parameters in order to evaluate its ability to deal with the different driving situations without the need to adapt the parameters. In (Zhang et al., 2018), the planner's flexibility is defined by how many different types of scenarios it can manage by just altering parameters rather than modifying the fundamental issue formulation or problem structures. In (Mouhagir et al., 2017), trajectory planning based on clothoid tentacles was adopted. Different combinations for cost function weights were proposed and the results show that the proposed method was very sensitive to parameter variation and some combinations were not suitable for

real-time application. A study is presented in (Arnay et al., 2016) on the impact of the weights of a cost function with five criteria on the final behavior of the vehicle. This planner deals with only pedestrians as obstacles and low velocities. Several configurations were chosen and ranked based on two behaviors.

In order to choose the best combination of weights, the role of each cost must be investigated and its influence in choosing the best candidate trajectory must be understood. In this paper, impact analysis and tuning of weighting coefficients are done on the planning algorithm presented in (Said et al., 2021). This paper is organized as follows: in Section 2, we present the trajectory planning algorithm. The global cost function and its components are detailed in Section 2.2. Section 3 presents the proposed method and reports the simulation results with some analysis on the cost weights, while the final Section 4 concludes the paper.

# 2 TRAJECTORY PLANNING

## 2.1 Presentation of the trajectory planning method

The trajectory planning algorithm must provide the best trajectory from a set of candidate trajectories that helps the vehicle to track a reference trajectory while avoiding static and mobile obstacles and ensuring safety and passenger comfort. Fig.1 shows the local trajectory planning module. Starting from matching the vehicle on the reference trajectory, a set of candidate trajectories are generated. they cover either the host lane or the entire width of the road depending on their navigability. Each of them consists of two phases: The transient phase, which is modeled by a $4^{th}$ order polynomial curve to provide a smooth change ensuring continuity of the curvature, starts at the actual position of the vehicle up to a defined lateral offset from the reference trajectory. Then, the candidate trajectory continues with a permanent phase parallel to the reference trajectory where the lateral offset becomes constant (see Fig. 2). Secondly, an obstacle detection procedure is carried out. A classification area is formed along the candidate trajectory by the footprint of the vehicle. The collision distance $d_{obs}$, which is the free distance traveled on the trajectory to reach the first obstacle, is then detected. Based on the collision distance and security distance, we classify the candidate trajectories into three classes: non, partially, or fully navigable trajectory. Note that the security distance is the distance the vehicle must maintain between it and the encountered obstacle. It depends on the obstacle state (static or dynamic). It is calculated based on the safe stop distance, the needed distance to stop the vehicle from its actual speed, with a defined comfortable deceleration. If there are no navigable trajectories, the algorithm selects the one with the longest distance to the obstacle to stop the vehicle with high deceleration (safe stop scenario). Thirdly, the navigable trajectories are evaluated according to various criteria, including smoothness, safety, consistency with the previously selected trajectory of the vehicle, and tracking of the reference center lane. All these costs are detailed in Section 2.2. Once these criteria are costed and merged into a weighted global cost function, the chosen trajectory is the best one with the lowest cost. Finally, a set of points, defined by the curvilinear abscissa, x and y coordinates, velocity, and curvature, depicts the best trajectory. For more details on the planning algorithm and its implementation, please refer to (Said et al., 2021).

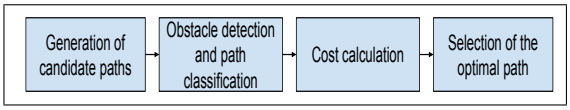


Figure 1: Local trajectory planning module

## 2.2 Cost function definition

The cost function is a weighted combination of costs that should be minimized in order to find the best trajectory among the many candidate trajectories generated by the planning algorithm. These costs are:

1. **Smoothness cost** $C_\rho[i]$
   This cost seeks to prefer lower-curvature trajectories. On the other hand, soft smoothness causes increased lateral acceleration, which affects passenger comfort. As a result, the integration of the curvature squared along a trajectory is chosen as a smoothness requirement for this trajectory in order to reduce its slackness:

$$C_\rho[i] = \int {\rho_M^i}^2 \, ds_M^i \tag{1}$$

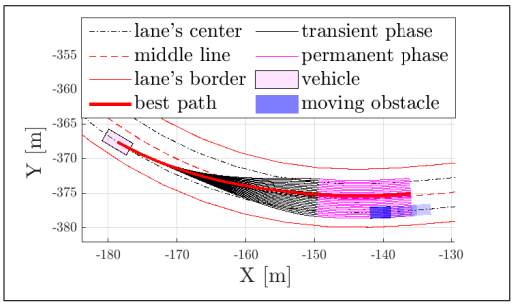


Figure 2: Trajectory planning: simulation environment

where $\rho_M$ and $ds^i_M$ are the curvature and the curvilinear abscissa of a point $M$ along the candidate trajectory $i$, respectively.

2. **Cost of tracking the reference trajectory $C_r[i]$:**
In order to position the ego vehicle in the center of the intended lane, the vehicle must follow the global reference trajectory. The cost of following the reference trajectory is related to the offset since the candidate trajectories are created around this lane center with a given lateral offset (Fig. 2). The reference cost in multi-lane structured environment is determined by the vehicle's position in relation to the lanes. So, the reference cost is given by:

$$C_r[i] = (q^i_f - q_{refc})^2, \tag{2}$$

where $q^i_f$ is the lateral shift of the permanent phase of the candidate trajectory $i$ to the host lane, $q_{refc}$ is the lateral offset of the center of the reference lane. By default, the reference lane is the one in which the vehicle is located: it is either the host lane ($q_{refc} = 0$) or adjacent lane ($q_{refc} = q_{L2}$). However, in case of returning to the host lane in an obstacle overtaking scenario, the host lane becomes the reference if the vehicle passes the obstacle (dotted lane in Fig.3) and the host lane is navigable. Fig.3 shows the different cases for the definition of the reference lane.

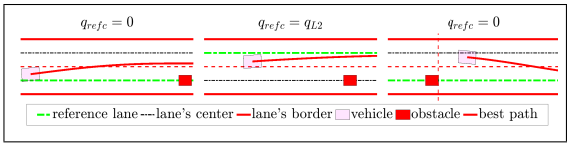


Figure 3: Reference cost cases

3. **Consistency cost $C_c[i]$:**
A quick shift in the selected trajectory between two iterations needs a considerable control effort and can affect the vehicle's stability. As a result, a measure of similarity between the prior trajectory and the current candidate trajectory is required to avoid generating a trajectory that is drastically different from that of the previous step. Our technique reduces it to the difference between the current trajectory index $i$ and the chosen one from a prior planning iteration.

$$C_c[i] = |i - i^{t-1}_{des}| \tag{3}$$

4. **Safety cost $C_s[i]$:**
We define two safety costs: a longitudinal cost $C_{sl}$ and a lateral cost $C_{sL}$. The first one assesses the trajectory's navigability and the distance to the first obstacle. This cost increases when the first detected obstacle is longitudinally close and decreases when the obstacle is far (Fig. 4-left). The second cost considers the navigability of nearby trajectories and attempts to position the vehicle laterally in the middle of the navigable zone. The collision distance $d_{obs}$ (distance to the first obstacle) is transformed into a safety cost as follows:

$$C_{sl}[i] = \begin{cases} 0 & \textit{obstacle-free trajectory} \\ 2 - \frac{2}{1+e^{-c_1\ d^i_{obs}}} & \textit{otherwise} \end{cases} \tag{4}$$

$$g[k] = \frac{1}{\sqrt{2\pi}\sigma}\ exp\left(-\frac{(k\ \Delta q)^2}{2\sigma^2}\right) \tag{5}$$

$$C_{sL}[i] = \left(\sum_{j\in\Gamma^i} C_{sl}[j]\ g[i-j]\right)/n_{\Gamma^i} \tag{6}$$

where $c_1$ is a cost setting parameter, $\Delta q$ is the desired lateral sampling resolution, $\sigma$ is the standard deviation of the discrete Gaussian convolution for the risk of collision and is calculated by considering that $g[\frac{L_v}{\Delta q}] = 0.5$, where $L_v$ is the vehicle width (Fig. 4-right). $\Gamma^i$ is the set of indexes of generated trajectories without $i$, $n_{\Gamma^i}$ is their number.

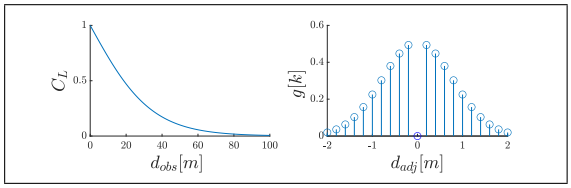


Figure 4: Safety cost

**Total cost function $C_T[i]$:**
We use the normalization technique to make the different cost criteria dimensionless because they are assessed in different units. As a result, we use the following formula:

$$\overline{C_.}[i] = \frac{C_.[i] - min(C_.)}{max(C_.) - min(C_.)} \tag{7}$$

Then, the total cost function $C_T[i]$ of a given trajectory is defined as the weighted sum of the normalized cost functions defined above:

$$\begin{aligned} C_T[i] =& W_\rho \overline{C_\rho}[i] + W_c \overline{C_c}[i] + W_r \overline{C_r}[i] \\ &+ W_{sL} \overline{C_{sl}}[i] + W_{sl} \overline{C_{sL}}[i] \end{aligned} \tag{8}$$

with $W_\rho$, $W_c$, $W_r$, $W_{sL}$ and $W_{sl}$ the weighting coefficients of smoothness, consistency, reference tracking, longitudinal safety and lateral safety costs respectively.

# 3 Impact analysis and tuning of weighting coefficients

## 3.1 Proposed method

Our goal is to understand better each cost influence on choosing the best trajectory and to find a generic weighting coefficients range for the cost function of the planning algorithm. First, we propose scenarios with or without static or dynamic obstacles. Second, we generate $n$ random combinations of weighting coefficients, each weight is bounded between two values ($0 \leq l_b \leq W_. \leq u_b \leq 1$). The random method was used due to the high number of combinations in a classic grid search method with five weights. Then, we run the planning algorithm $n$ times. The $n$ vehicle's trajectories obtained are classified into two categories:

- $T_c$ complete vehicle's trajectory set: the algorithm manages to reach the end of the proposed scenario without stopping or colliding with any obstacle.
- $T_i$ incomplete vehicle's trajectory set: the algorithm fails to reach the end of the proposed scenario due to hitting an obstacle or lane's borders.

The correlation between the obtained results and the corresponding combinations is then analyzed according to various factors such as the distance traveled, the longitudinal and the lateral acceleration, the reference tracking, the safety distance, and the overall behavior (conservative or aggressive). Based on this analysis, the wide range chosen first is contracted. this procedure is repeated until we obtain the desired generic range.

## 3.2 Case study

To study the proposed method, we apply the planning algorithm on a portion of a realistic trajectory track taken from *SCANeR*$^{TM}$ *studio* simulator, with different scenarios, for 50 random combinations. This trajectory and the corresponding limit speed and curvature are shown in Fig. 5. Initial speed may vary depending on the scenario. The trajectory planning module is implemented in an autonomous driving system composed of main modules for navigation: localization, perception, trajectory planning, control, and vehicle model. The two last modules are running at 50 Hz while the others are running at 10 Hz. The Renault-Zoe robotic vehicle model validated on *SCANeR*$^{TM}$ *studio* is used.

The presented scenarios are simulated using the combinations of weighting coefficients presented in Fig. 6. We start with simple scenarios and large ranges for weighting coefficients. The smoothness,

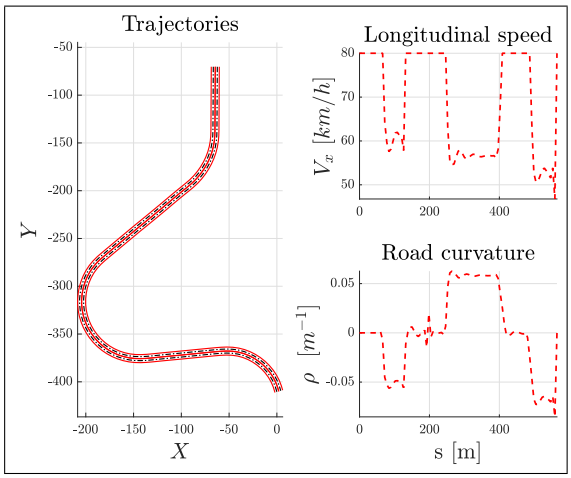


Figure 5: Trajectory, longitudinal speed and curvature (same legend as Fig. 2)

reference, and consistency coefficients ranges are chosen to be between 5% and 40% as they are used for performance purposes,while the coefficients ranges of safety costs are greater: The longitudinal safety one is between 5% and 65%. The lateral safety one is between 5% and 50%. These ranges are chosen based on evident knowledge about the algorithm and preliminary simulations. Safety is prior to performance while deciding the trajectory for autonomous navigation. Outside of these ranges, the planning algorithm does not give reasonable trajectories that can be executed. It will either give an extremely smooth with high smoothness weight or aggressive trajectory with high reference weight that will try to follow the lane's center.

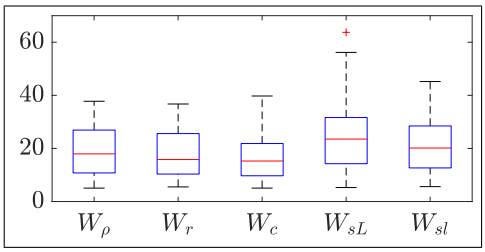


Figure 6: Box plot of 50 combinations of weighting coefficients

In the following, for each scenario, we illustrate the generated trajectories for all combinations and the final reached points for the same time horizon in order to analyze the results.

### 3.2.1 Scenario 1: static obstacle overtaking

The scenario presented in Fig. 7 consists of an overtaking of two static obstacles, each one on a lane sep-

arated by a distance of $15m$. This distance is considered small, taking into account the lane's desired speed ($65km/h$), and for this, the algorithm pushes the vehicle to brake when it slaloms between obstacles.

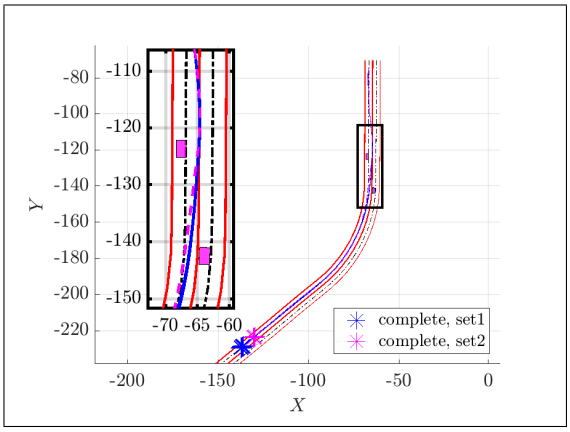


Figure 7: Scenario 1: trajectories in presence of 2 static obstacles (same legend as Fig. 2)

In some combinations, where the sum of smoothness and consistency weights is significant (Set 2: $W_\rho > 12\%$ or $W_c > 13\%$ ), the vehicle crosses the trajectory with a high lateral acceleration value ($> 4m/s^2$) as shown in set 2 in Fig. 8, where set 1 represents trajectories with the remaining combinations. The smoothness cost leads the vehicle to move

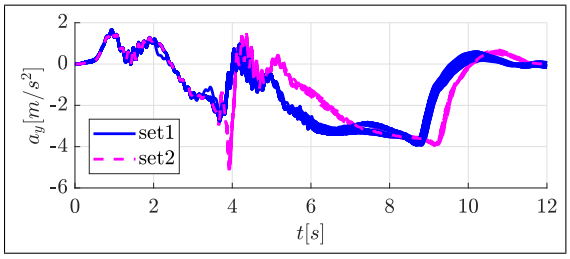


Figure 8: Scenario 1: lateral acceleration

straight towards the obstacle, especially if the longitudinal safety weighting coefficient is too small. In contrast, the consistency cost delays the lane change until the last possible moment before reaching the safe stop distance, and this results in strong lateral acceleration. Then the algorithm proceeds to additional braking to ensure lateral stability. We note here that the developed algorithm is able to execute the trajectory safely, even with small safety weighting coefficients. As we can see in Fig. 7, all trajectories can reach the end of the scenario, and with almost a $10m$ difference between their ends due to additional braking on some trajectories (set 2). However, we can note that the trajectories with high lateral safety ($W_{sl} > 40\%$) and reference ($W_r > 20\%$) weighting coefficients execute the longest distance and hence offers the highest longitudinal speed.

### 3.2.2 Scenario 2: Mobile obstacle overtaking

The second scenario is a simple overtaking of a mobile obstacle at $40km/h$ where the vehicle speed during overtaking reaches 50 to $60km/h$. As we can see in Fig. 9, all trajectories can reach the end of the scenario.

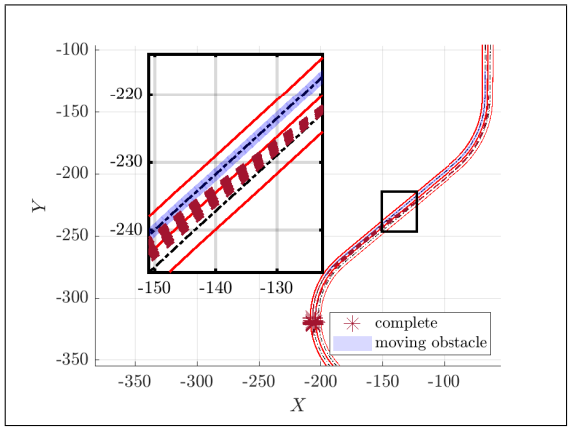


Figure 9: Scenario 2: trajectories in a mobile obstacle overtaking (same legend as Fig. 2)

The difference between trajectories can be seen in Fig. 10 when overtaking and returning to the host lane. The security inter-distance is respected in all combinations but leads to more or less conservative behavior depending on the reference weighting coefficient. For all combinations, the vehicle starts overtaking before $35m$, which is the security distance corresponding to its velocity. However, the overtaking starts earlier with a high lateral safety weight. However, when returning to the lane, the inter-distance of the first trajectory that reaches the host lane's center is equal to $22m$, which is equal to 2 seconds of obstacle's speed. Set 4 in Fig.10 represents trajectories with smoothness weight $W_\rho$ higher than $> 30\%$. In this set, the three trajectories with a late return to the lane have in addition a low reference weight $W_r < 7\%$, while the rest of the trajectories try hard to follow the center of the track. Furthermore, the reference cost acts on the vehicle stability: a high reference weight with low smoothness or consistency weight (set5: $W_r > 15\%$ and ($W_\rho < 6\%$ or $W_c < 6\%$) ) leads to a higher lateral acceleration compared to other combinations (see Fig.11) and may result in a passenger's discomfort, due to late change lane and rapid return to the host lane. Note that set 3 represents trajectories with the remaining combinations.

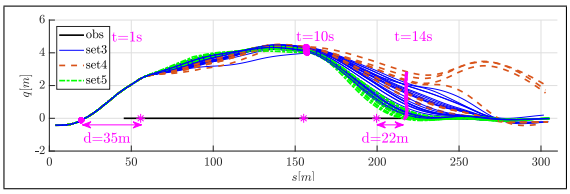


Figure 10: Scenario 2: Frenet frame

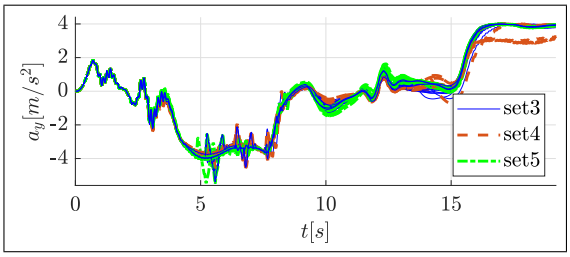


Figure 11: Scenario 2: lateral acceleration

### 3.2.3 Scenario 3.1: multi-maneuver scenario

This scenario combines several maneuvers: reference tracking, tight passage, static obstacle overtaking with a mobile obstacle on the adjacent lane in the opposite direction ($t = 10s$), and mobile obstacle overtaking ($t = 20s$).

As we can see in Fig.12, 92% of the generated trajectories can complete the scenario. The incomplete trajectories fail at the tight passage: the classification area around the trajectory, which is a little larger than the vehicle's imprint, detects hitting one of the obstacles. The four failed combinations have low lateral safety weights ( $W_{sl} < 10\%$) value and high reference weight ($W_r > 30\%$). This result is expected as the reference cost forces the vehicle to track the reference lane while the lateral safety cost tries to pass it in the middle of the navigable zone.

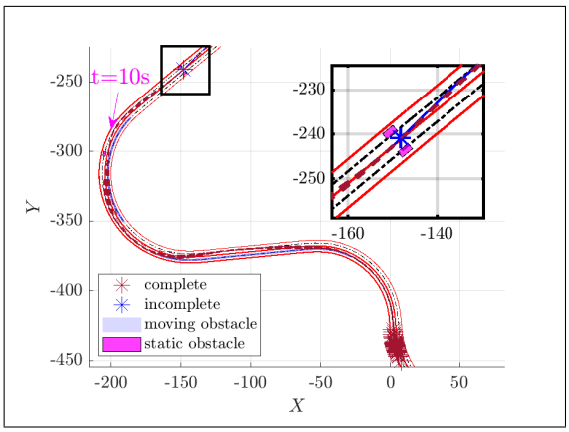


Figure 12: Scenario 3.1: trajectories (same legend as Fig. 2)

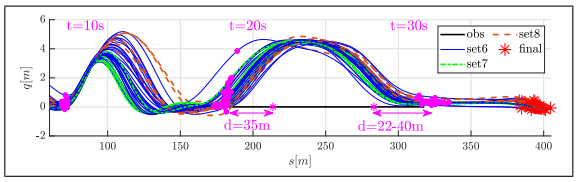


Figure 13: Scenario 3.1: Frenet frame

Fig.13 represents the generated trajectories in the Frenet frame. We can see a significant difference between the trajectories. After $t = 10s$, we notice that a high reference and lateral safety weights (set 7: $W_r > 18\%$ and $W_{sl} > 30\%$) lead to an early return to the host lane, while those with low reference weight and high smoothness weights (set 8: $W_r < 8\%$ and $W_\rho > 25\%$) were late to return and overtake. In addition, the last one to return was the one with a high value of smoothness weight ($W_\rho = 39\%$) and caused over-steering when trying to follow the reference ($s = 170m$). At the overtaking of the mobile obstacle ($t = 20s$), the high lateral safety weight leads to earlier overtaking and then to an earlier return to the lane. The longest trajectories were those with the high lateral safety weight ($W_{sl} = 45\%$ of the longest one). Note that set 6 represents trajectories with the remaining combinations.

| cost | result |
|---|---|
| $W_\rho$ | high value of smoothness weight leads to a late lane change, high $a_y$ and over/under steer |
| $W_r$ | high value of reference weight leads to an early lane change, high $a_y$, prioritize reference tracking over safety |
| $W_c$ | high consistency weight leads to high $a_y$ ($> 0.4g$) |
| $W_{sL}$ | high lateral safety weight leads to longest path, early lane change; |
| $W_{sl}$ | longitudinal safety weight has a similar effect to lateral safety ; |

Table 1: Cost analysis results

From these results, we can deduce that the smoothness, reference, and consistency weighting coefficients should be limited to relatively small values. Indeed, a high reference weight coefficient can be aggressive in a dual lane change scenario. Furthermore, high smoothness and consistency weights may cause a delay in response to the change in curvature. Consequently, bounded combinations are applied in the following simulation scenario.

### 3.2.4 Scenario 3.2: multi-maneuver scenario with limited combinations

After many tests and simulations, we decided to limit the ranges of weighting coefficients around the most favorable values. The new range proposed for combinations of weighting coefficients is between 5% and 10% for smoothness and consistency cost's weights, between 5% and 15% for reference cost's weight, and between 15% and 65% for longitudinal and lateral safety cost's weights. These new ranges are applied to the same scenario of 3.2.3. As we can see in Fig. 14, all trajectories can reach the end of the scenario, and the difference at the arrival point is less than $5m$ for different combinations of trajectories. In addition, it shows that all trajectories can pass smoothly and follow the reference without any accident.

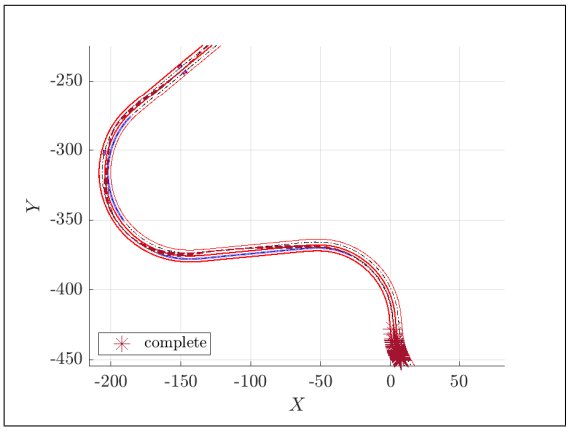


Figure 14: Scenario 3.2: trajectories (same legend as Fig. 2)

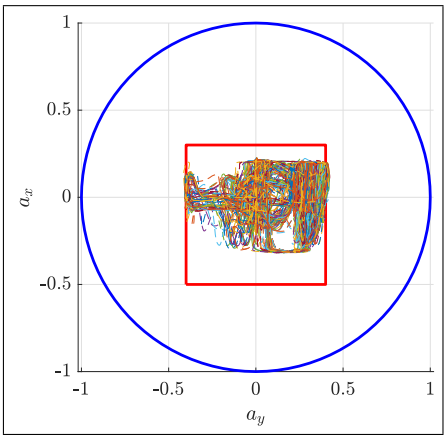


Figure 15: g-g diagram for 50 combinations in a 0.4g red box

Using a normalized friction circle and the g-g diagram, we show that the planning algorithm can maintain the vehicle for all combinations in the comfort region (red rectangle in Fig.15). A classification of combinations based on maximal lateral acceleration reached with a threshold of $0.38g$ is done. The results are illustrated using the box plot shown in Fig.16: A high lateral acceleration is reached with a low lateral safety weight and a high reference weight. This behavior is expected due to the late lane change. Note that even the combinations presenting high lateral acceleration values still have an acceleration less than $0.4g$ as shown in Fig.15.

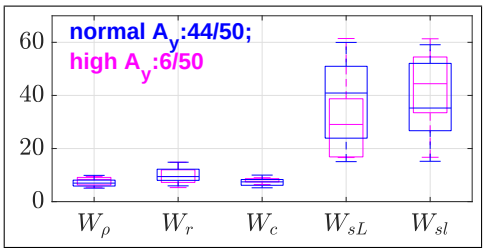


Figure 16: Box plot of combinations of weighting coefficients

Note that these combinations are simulated for all the previous scenarios and succeed in reaching their ends.

### 3.2.5 Scenario 3.3: longitudinal and lateral safety costs

To better understand the impact of the two components of the safety cost of the algorithm behavior, we simulate the third scenario with a fixed value for smoothness, reference, and consistency weights as 8%, 14% and 8% respectively, while the range of the two safety costs is between 15% and 65%. All combinations succeed in finishing the scenario smoothly with a lateral acceleration inside the comfort zone.

## 3.3 Discussion about costs influence correlation

The results presented above give us a better understanding of the different costs that influence choosing the best trajectory. These simulations helped us to improve the planning algorithm. A good combination weight coefficients leads the vehicle to track the reference lane and to overtake smoothly and safely in the presence of obstacles, when overtaking is possible, without an abrupt lane change. Moreover, the planning algorithm respects the safety distances with all static and mobile obstacles and stops the vehicle if needed when no navigable trajectory is detected.

The smoothness cost, as defined, tries to move the vehicle straight forward as much as possible. Unfortunately, it delays the lane return with low reference cost or high consistency cost. The consistency cost acts as a damper of the vehicle's motion by delaying the variation of the vehicle's orientation. Concerning the reference cost, it plays an essential role, as presented before in all the scenarios. When encountering an obstacle, a high reference weight causes a high lateral acceleration, especially for the combination where the consistency or smoothness weight is low or the lateral safety weight is low. The safety cost guides the vehicle very well in the navigable zone and respects the inter-distances. In some cases, the costs identified above may correlate with each other. For example, in the case of lane following, the lateral safety cost correlates with the reference tracking cost by maximizing the lateral safety cost of candidate trajectories near the lane borders and thus minimizing those towards the lane's center. On the other hand, they behave differently when the lateral safety cost tries to position the vehicle in the middle of the navigable zone, away from the reference lane. The higher is the reference cost; the earlier is the host lane tracking. Finally, choosing the different weights of the cost function components must obey to a compromise between the other considered criteria. It is crucial to prioritize safety on performance. The present analysis shows that the proposed planning algorithm is robust against the cost weights variation. Moreover, this study allows us to identify the more suitable ranges for the different weights to arrive to a robust combination. Hence, the objective is to arrive to a planning algorithm tuning as generic as possible to the variation of driving conditions in a dynamic environment. The combination 8%, 14%, 8%, 40%, and 30% for smoothness, reference, consistency, longitudinal and lateral safety weights, respectively, is adopted as being a good compromise between safety and performance.

## 4 Conclusion

In this paper, after presenting briefly the local trajectory planning method developed, we have introduced the method used to determine, analyze and fine tune the best ranges of the different weights of the trajectory planning cost function. The planning algorithm is tested using a variety of scenarios and ranges of weights combinations. This study shows the role of each cost in determining the best overall trajectory and leads us to select a range for each cost weight. We can conclude that the planning algorithm is robust to the variation of the cost weighting, which represents a significant advantage for encountering various driving situations and conditions in a dynamic environment, without the need for re-adjusting and tuning the planning algorithm.

## REFERENCES


Alia, C., Gilles, T., Reine, T., and Ali, C. (2015). Local trajectory planning and tracking of autonomous vehicles, using clothoid tentacles method. In *2015 IEEE intelligent vehicles symposium (IV)*, pages 674–679. IEEE.

Arnay, R., Morales, N., Morell, A., Hernandez-Aceituno, J., Perea, D., Toledo, J. T., Hamilton, A., Sanchez-Medina, J. J., and Acosta, L. (2016). Safe and reliable path planning for the autonomous vehicle verdino. *IEEE Intelligent Transportation Systems Magazine*, 8(2):22–32.

Dixit, S., Fallah, S., Montanaro, U., Dianati, M., Stevens, A., Mccullough, F., and Mouzakitis, A. (2018). Trajectory planning and tracking for autonomous overtaking: State-of-the-art and future prospects. *Annual Reviews in Control*, 45:76–86.

Karaman, S. and Frazzoli, E. (2011). Sampling-based algorithms for optimal motion planning. *The international journal of robotics research*, 30(7):846–894.

Katrakazas, C., Quddus, M., Chen, W.-H., and Deka, L. (2015). Real-time motion planning methods for autonomous on-road driving: State-of-the-art and future research directions. *Transportation Research Part C: Emerging Technologies*, 60:416–442.

Lim, W., Lee, S., Sunwoo, M., and Jo, K. (2018). Hierarchical trajectory planning of an autonomous car based on the integration of a sampling and an optimization method. *IEEE Transactions on Intelligent Transportation Systems*, 19(2):613–626.

Mouhagir, H., Cherfaoui, V., Talj, R., Aioun, F., and Guillemard, F. (2017). Trajectory planning for autonomous vehicle in uncertain environment using evidential grid. *IFAC-PapersOnLine*, 50(1):12545–12550.

Pivtoraiko, M. and Kelly, A. (2005). Efficient constrained path planning via search in state lattices. In *International Symposium on Artificial Intelligence, Robotics, and Automation in Space*, pages 1–7. Munich Germany.

Said, A., Talj, R., Francis, C., and Shraim, H. (2021). Local trajectory planning for autonomous vehicle with static and dynamic obstacles avoidance. In *2021 IEEE International Intelligent Transportation Systems Conference (ITSC)*, pages 410–416. IEEE.

Zhang, Y., Chen, H., Waslander, S. L., Yang, T., Zhang, S., Xiong, G., and Liu, K. (2018). Toward a more complete, flexible, and safer speed planning for autonomous driving via convex optimization. *Sensors*, 18(7):2185.